

Illuminating the Lateral Organization of Cell-Surface Proteins CD24 and CD44 through Plasmon Coupling between Au Nanoparticle Immunolabels

Xinwei Yu, Jing Wang, Amin Feizpour, Björn M. Reinhard

Department of Chemistry and The Photonics Center, Boston University, Boston, MA 02215, United States

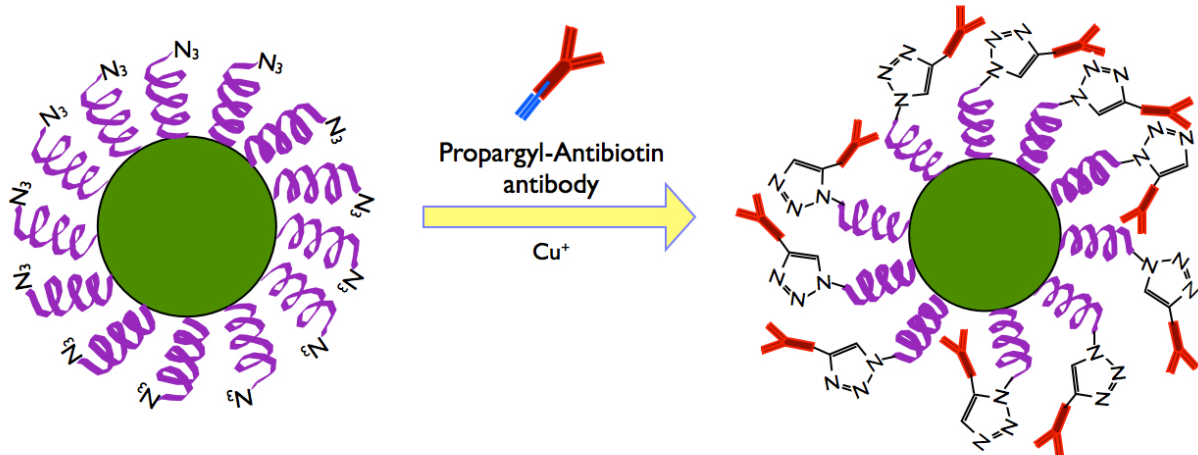


Figure S1. Schematic illustration of the NP functionalization through click chemistry. For Neutravidin functionalized gold nanoparticles, the antibiotin antibody was substituted by Neutravidin (see Methods).

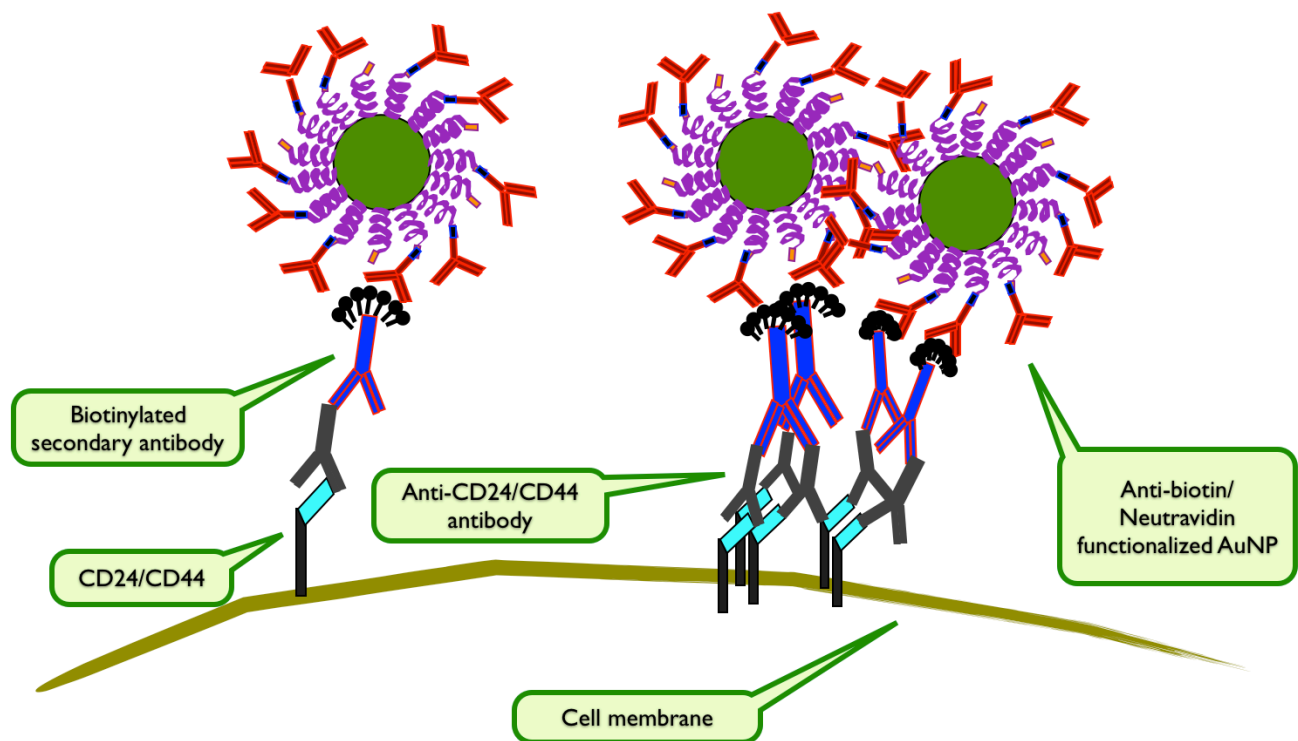


Figure S2. Schematic illustration of immunolabeling strategy of CD24 and CD44 on cell membrane. Anti-CD24/CD44 antibody, biotinylated secondary antibody, and anti-biotin/Neutravidin (in the experiment of extraction of cholesterol) functionalized AuNPs were applied onto cell membrane surface successively (see Methods).

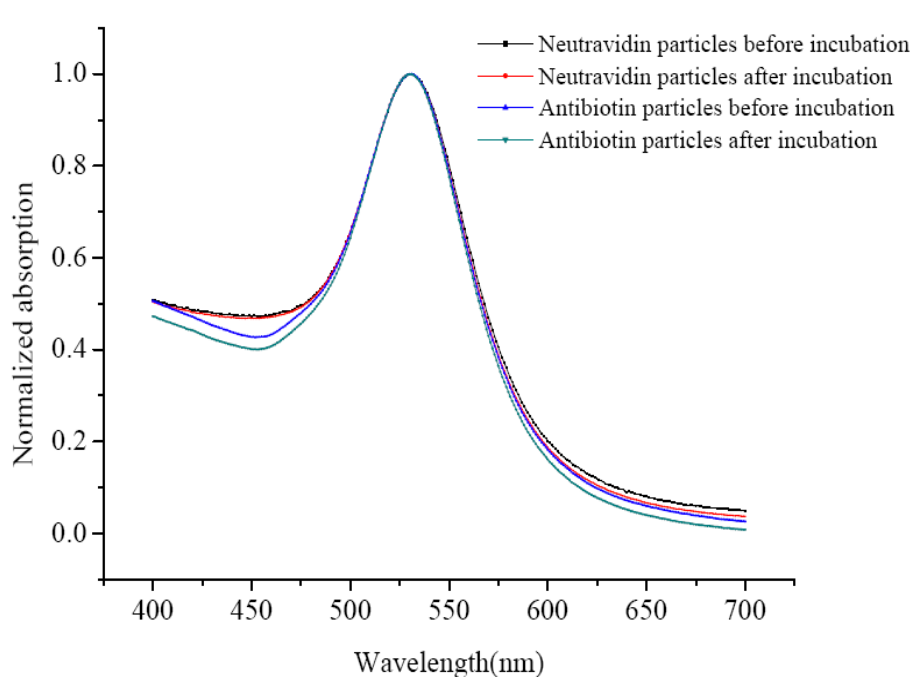


Figure S3. UV-VIS absorption spectra of antibody functionalized Au NPs before and after incubation with the cells. The peak wavelengths remains at 530nm, confirming the excellent stability of the functionalized NPs.

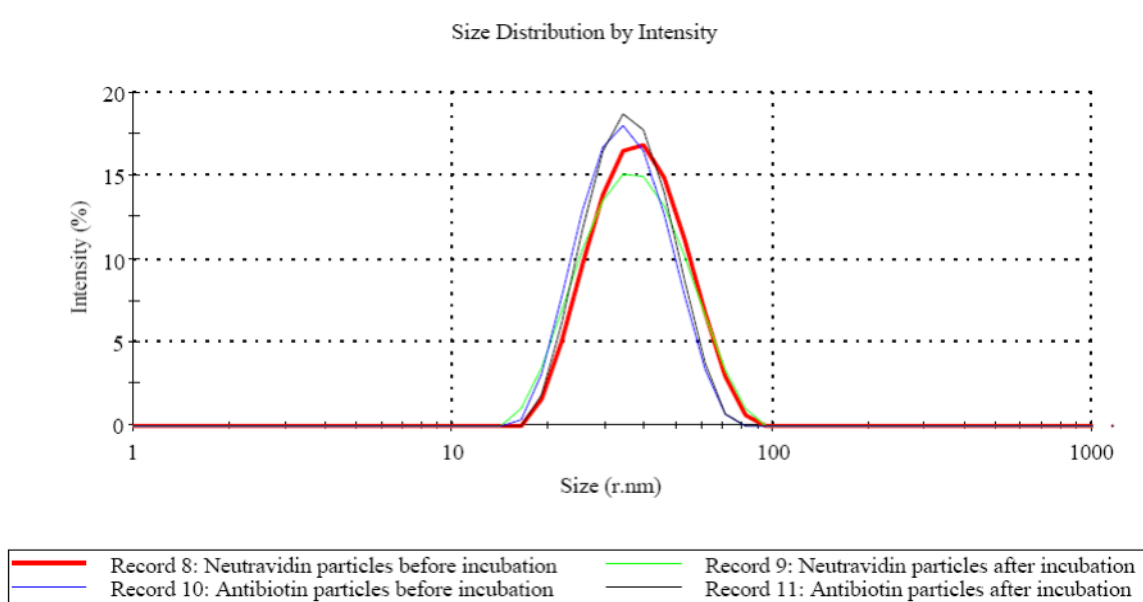


Figure S4. Size distribution of functionalized NP immunolabels before and after incubation with cells by dynamic light scattering. The size distributions all center at a radius of approx. 30nm, which confirms the stability of the functionalized NPs.

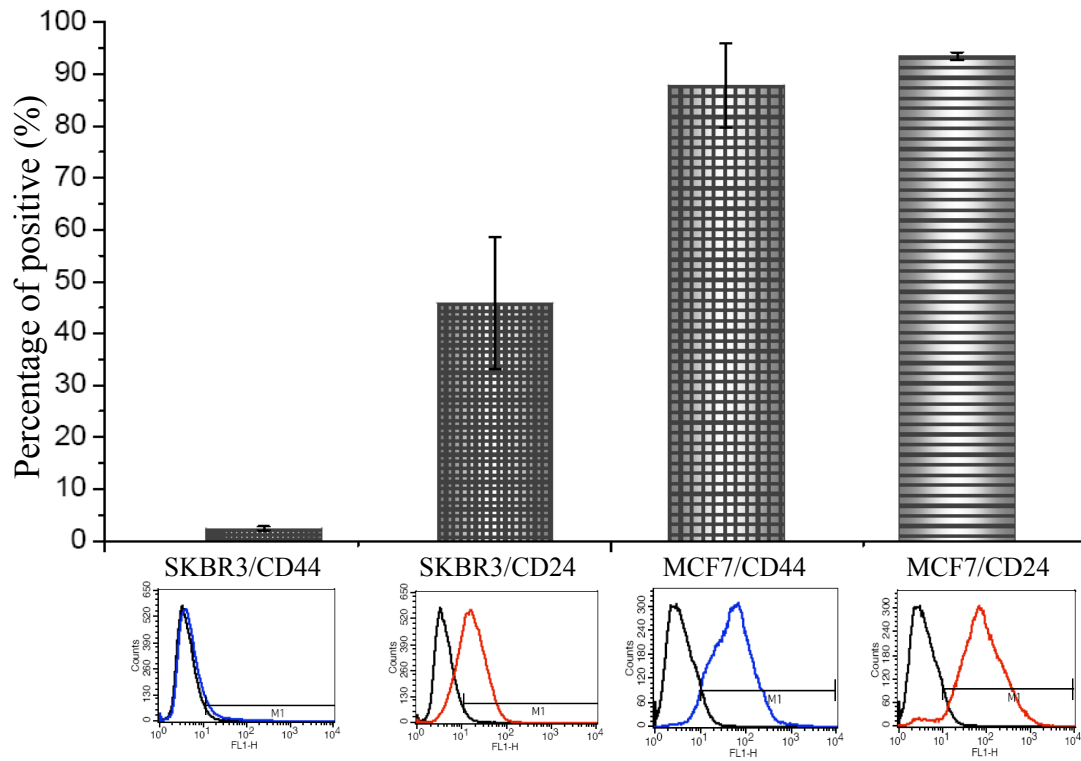


Figure S5. Characterization of expression levels of CD24 and CD44 on MCF7 and SKBR3 cell lines via flow cytometry. MCF7 cells overexpress both CD24 and CD44. SKBR3 cells only overexpress CD24. The expression level of CD44 is low.

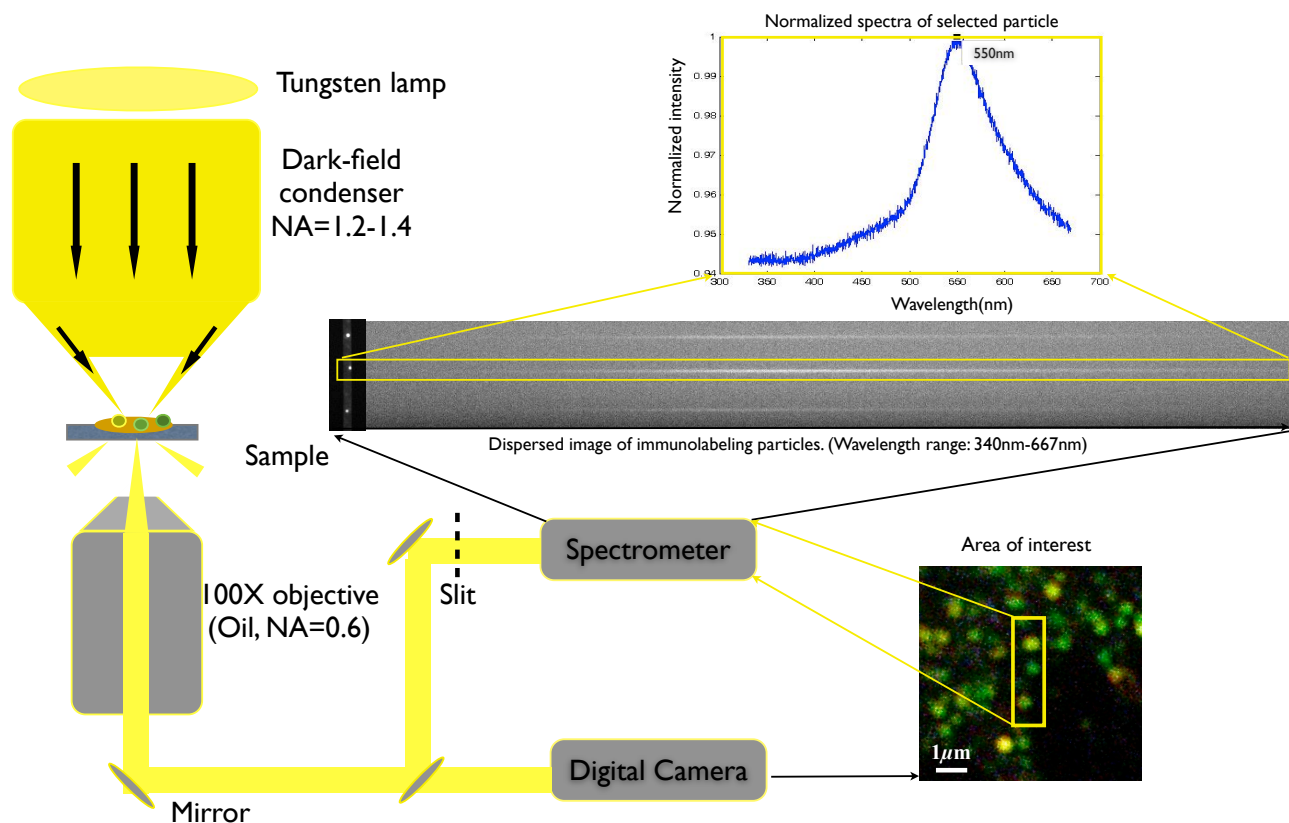


Figure S6. Spatially resolved spectrum acquisition. a) Optical set-up. The NP labeled cell surfaces were illuminated by a tungsten light source (100W) via a dark-field oil condenser (NA = 1.2-1.4). The microscope was equipped with a 100X oil objective (NA=0.6). Scattering images were collected through an eyepiece adapter using an Olympus SP310 digital camera. b) After identification of individual scatterers on the cell surface in the recorded images, scattering spectra of selected emitters were recorded using an Andor spectrometer connected to the microscope. A controllable entrance slit in combination with the spectrometer acquisition software allowed the selection of individual scatterers for data acquisition. The entrance slit of the spectrometer was set to 2µm.

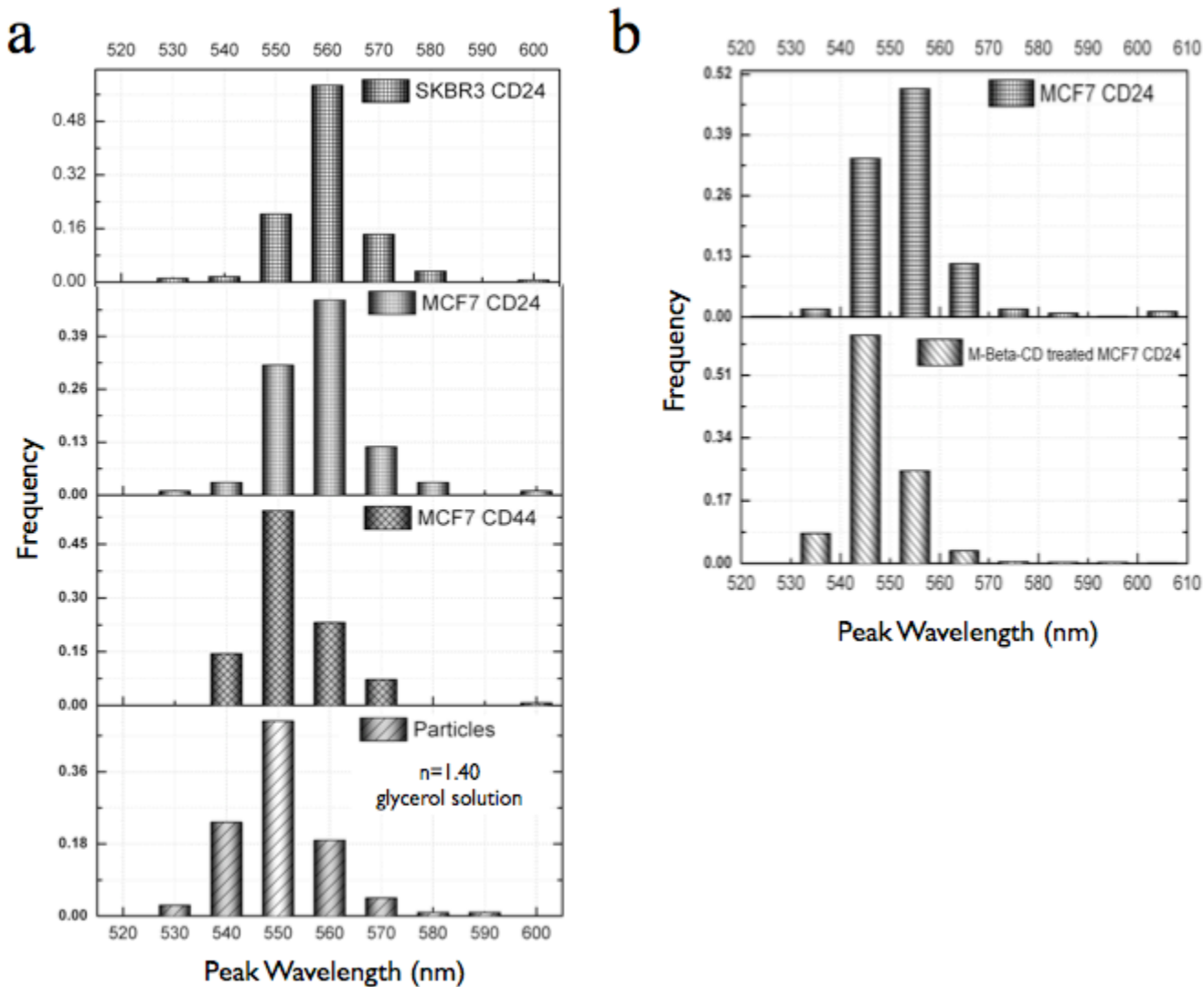


Figure S7. Distribution of cluster peak wavelengths of a) NP immunolabels targeted at (top to bottom) SKBR3/CD24, MCF7/CD24, MCF7/CD44 and randomly deposited NPs covered with a glycerol solution ($n_r = 1.40$), and b) NP immunolabels targeted at MCF7/CD24 before (top) and after (bottom) treatment with beta-cyclodextrin. The histograms show that both CD24 and CD44 are organized into clusters (indicated by the red-shifted peak wavelengths) on MCF7 and SKBR3 and that CD24 tends to form larger clusters than CD44. The blue-shift in the spectra of MCF/CD24 after treatment with beta-cyclodextrin in b) is consistent with a removal of the preferential CD24 clustering upon lipid raft disruption due to cholesterol sequestration.

Number of NPs	Au-NP	Standard deviation	MCF7 CD44	Standard deviation	MCF7 CD24	Standard deviation	SKBR3 CD24	Standard deviation
1	91.8%	1.90%	57.0%	5.78%	35.6%	6.51%	62.5%	5.35%
2	7.38%	1.00%	20.0%	0.416%	19.4%	2.69%	20.3%	0.324%
3	0	0	4.17%	2.04%	9.12%	0.994%	4.44%	2.49%
4	0	0	0.728%	0.566%	4.06%	0.564%	2.87%	1.18%
5	0.561%	0.559%	9.81%	2.65%	10.3%	1.85%	4.54%	1.45%
Clusters with more than 6 NPs	0.261%	0.452%	8.26%	6.85%	21.6%	9.62%	5.30%	3.30%

Table S1. Cluster size distributions of CD24 and CD44 on MCF7 and SKBR3 cells. For each cell line/receptor combination, 1500-2500 particles were evaluated from 13 randomly chosen cell samples using SEM.

Number of NPs	Normal MCF7 CD24	Standard deviation	m-beta-CD treated MCF7 CD24	Standard deviation
1	42.2%	4.36%	82.9%	2.66%
2	20.5%	2.57%	11.2%	2.92%
3	7.41%	1.52%	4.34%	9.37%
4	3.29%	0.730%	0	0
5	11.3%	2.72%	0.613%	1.06%
Clusters with more than 6 NPs	15.2%	8.78%	0.858%	1.49%

Table S2. Cluster size distribution of CD24 on MCF7 cells with and without m- β -CD treated treatment. Neutravidin functionalized NPs were used in this experiment. . For each cell/receptor pair, more than 2000 particles were evaluated from 20 randomly chosen samples.

METHODS

Cell Culturing

SKBR3 cells were cultured in McCoy medium supplemented with L-glutamine, penicillin and streptomycin in a 5% CO₂ containing atmosphere at a relative humidity of 95% at 37°C. MCF7 cells were cultured in EMEM medium supplemented with 0.1% insulin, L-glutamine, penicillin and streptomycin under the same conditions. Cells to be immunolabeled were seeded either on glass coverslips or silicon substrates, and were grown to approximately 30% confluency.

Immunolabeling

Functionalization of 40nm Au particles with propargyl-PEG-anti-biotin followed the procedure described previously^{1,2}. Briefly, 5ul of 10mM thiol-PEG-azide solution (Nanocs, MW 3400) was incubated with 40nm AuNPs (TedPella, ~9x10 particles/mL) overnight at room temperature, followed by three centrifugation (5500rpm, 10min) washing steps using distilled deionized (ddi) water. In the meantime, 2uL of 100mg/mL propargyl-PEG-NHS ester (Quanta design) DMSO solution was mixed with 100uL of 1mg/mL anti-biotin antibody (Sigma-Aldrich) in 1x PBS (pH 7.2) in ice bath for 6 hours. Excess propargyl-PEG-NHS ester was removed using a 7K MWCO size exclusion column. 100uL propargyl-PEG-anti-biotin antibody was then incubated with 20uL PEG-AuNPs in the presence of click chemistry catalyst (a mixture of 100 nmol ascorbic acid and 20 nmol CuSO₄ in ddi water) at 4°C for 8 hours. The particles were then washed three times by centrifugation (4500rpm, 10min, ddi water), resuspended in 0.5x PBS, pH 7.2, and used immediately afterwards. Neutravidin functionalized Au-NPs were obtained using the same approach but replacing anti-biotin antibody with Neutravidin.

SKBR3 and MCF7 cells grown on glass coverslips or silicon substrates were briefly rinsed with 10ml 1x HBSS buffer at 37°C. The cells were then fixed by immersion in 4% formaldehyde solution for 10min at room temperature, followed by three times of immersion into ice-cold 1x PBS for 5 min. Subsequently, the cells were blocked by incubation with 1% BSA at 4°C in 1x PBS for 1 hour.

Primary antibodies against CD44 or CD24 (Invitrogen) were diluted to 1:1000 in 1x PBS, then applied onto the cell slides prepared above. After incubation for overnight at 4°C, the cells were washed three times by ice-cold 1x PBS for 5min each. Then the biotin-labeled secondary IgG antibody (1:1000 in 1x PBS) was added and incubated for 1 hour at room temperature. After three times of washing with ice-cold 1x PBS the cells were ready for NP immunolabeling.

400ul of the above functionalized Au NPs were incubated with each cell slide for 3 hours at room temperature in a water-vapor-saturated atmosphere. Then the cells were rinsed with copious amounts of ice-cold 1x PBS for three times. For Figures 1, 2, 3(a) and Figure 4, antibiotin functionalized Au-NPs were used; while for Figure 3 (b) and 5, Neutravidin functionalized Au-NPs were used as immunolabels.

The samples on glass coverslips were ready for optical inspection in the microscope after covering with a glass coverslip. The samples on silicon substrates were briefly immersed into ddi water to remove the salt on the surface, and then gently blow dried in a nitrogen stream. The samples were immediately imaged via Scanning Electron Microscopy (SEM).

To check the stability of the NP immunolabels under the chosen experimental conditions, we collected the functionalized NP immunolabels after their incubation with the cells and randomly deposited them onto a clean glass slide for 1 min. Then, the surface immobilized NPs were washed by rinsing with copious amounts of ddi water, after which a 51% glycerol solution with $n_r = 1.40$ was applied onto the NPs. This refractive index was chosen as average of the refractive indices of water and lipid membranes to simulate the ambient medium at the water/lipid bilayer interphase³. For the preparation of SEM samples the controls were prepared on silicon substrates in the same way but the addition of glycerol solution was omitted.

Microscopy

Darkfield Microscopy

An inverted microscope (Olympus IX71) with a high numerical aperture (NA) oil condenser (NA=1.2-1.4) was used to visualize the particle distribution of the samples prepared above. Images were taken with a 100x oil objective (NA=0.6) or 60x oil objective (NA=0.65). Color images were recorded with an Olympus SP310 digital camera connected to the microscope through an eyepiece adapter. A 100W tungsten lamp was used for illumination.

Spectroscopy

Darkfield spectroscopy was carried out with a 500 mm focal length imaging spectrometer (Andor Shamrock with Andor Newton electron multiplying charge coupled device (EMCCD) detector) attached to the darkfield microscope. The sample was illuminated with a 100 W Tungsten lamp and the scattered light was collected by 100x oil objective lens (Olympus, NA=0.6).

Data Acquisition

To obtain the individual cluster spectra, we firstly adjusted the slit of the spectrometer to be 2 μ m, so that only individual cluster spots were exposed to excitation light along x direction. The height of the individual cluster images on the EMCCD chip (i.e. along y direction) was determined by software control. The grating of the spectrometer was centered at 500nm and the monitored wavelength range was 340nm to 667nm. The dispersed images of individual clusters on the cell membranes were then recorded, with exposure time of 0.3s and 30 accumulations. The recorded scattering spectra were processed with a home-written Matlab code. Equally sized areas in direct vicinity of the individual clusters without NP labels served as background and were subtracted from the raw data. Dispersed images of 200nm polystyrene beads were recorded under identical conditions and were used to correct the spectra for the excitation profile of the Tungsten lamp. The same experimental approach was applied to record spectra of Au NPs in an ambient medium of $n_r=1.40$. All spectra were acquired in peripheral cell regions where the overall signal-to-noise ratio was the highest.

Cluster Size Analysis via SEM

SEM images of NP labeled cell surfaces were acquired at a magnification of $\sim 33k\times$. 10 pixels (~ 2 nm) were chosen as the threshold to define a cluster: if a particle had a distance of less than 10 pixels with any of the particles in one cluster, then this particle belonged to this cluster, and the size of this cluster increased by 1. In this way, each SEM image generated a cluster size distribution. To calculate cluster size distributions we averaged over at least 13 independent cell samples. To calculate error bars in the cluster size distributions, we broke the total amount of SEM images into three subsets and calculated the error as standard deviation of the average cluster sizes of the subsets.

Bibliography

1. Wang, J.; Boriskina, S. V.; Wang, H.; Reinhard, B. M. *ACS Nano* **2011**, 5, (8), 6619-6628.
2. Wang, H. Y.; Rong, G. X.; Yan, B.; Yang, L. L.; Reinhard, B. M. *Nano Lett* **2011**, 11, (2), 498-504.
3. van Manen, H. J.; Verkuijlen, P.; Subramaniam, V.; van den Berg, T. K.; Roos, D.; Otto, C. *Biophys J* **2008**, 94, (8), L67-L69.